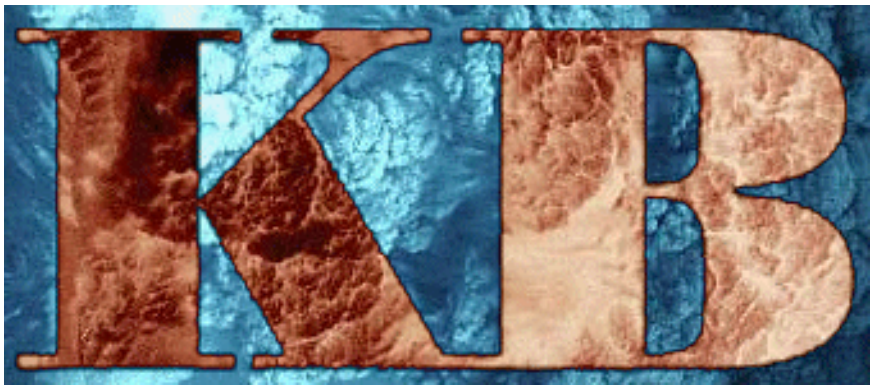

Physics of the KB codes

Field Precision

PO Box 13595, Albuquerque, New Mexico 87192
Telephone: 505-296-6689 FAX: 505-294-0222
E Mail: techinfo@fieldp.com Internet: www.fieldp.com

Section 1. One-dimensional equations of hydrodynamics

The hydrodynamic equations used in **KB1** are difference representations of conservation of mass, momentum and energy applied over elements[1]. Figure 1.1 shows element divisions for a one-dimensional simulation. Depending on symmetry, the slices represent thin plates, cylindrical shells, or spherical shells. The two sets of indices shown apply to elements and element boundaries (vertices). Boundary quantities are denoted with upper case letters and element quantities with lower case. For example, Element *i* with average radius r_i has boundaries at R_{i-1} and R_i. Elements retain their material identity as they move and change size during the calculation. The method is similar to Lagrangian finite-difference calculations[2]. An inherent limitation of the approach is the difficulty of modeling processes like mixing. On the other hand, the element-centered approach has two advantages:

- Automatic zone refinement for compressional phenomena like shocks.
- Ability to model explosive processes where the solution volume size may change by orders of magnitude.

In this discussion we shall concentrate on cylindrical systems. The extension to planar and spherical systems is straightforward. Conservation of mass implies that element masses do not change during the simulation. Consider an element with initial boundaries R_{oi-1} and R_{oi} and initial density ρ_{oi}. The mass is given by

$$m_i = \rho_{oi} \pi (R_{oi}^2 - R_{oi-1}^2). \tag{1.1}$$

The boundaries move in response to forces. The density at any time is related to the boundary positions by

$$\rho_i = \frac{m_i}{\pi (R_i^2 - R_{i-1}^2)} . \tag{1.2}$$

Note that Eqs. 1.1 and 1.2 do not employ approximations based on small element width. This feature avoids numerical problems when elements compress to cylindrical or spherical axes. Furthermore, the model allows the use of large elements. The average element radius corresponds to the center-of-mass coordinate. Assuming a uniform density, the average radius of a cylindrical element is related to the boundary radii by

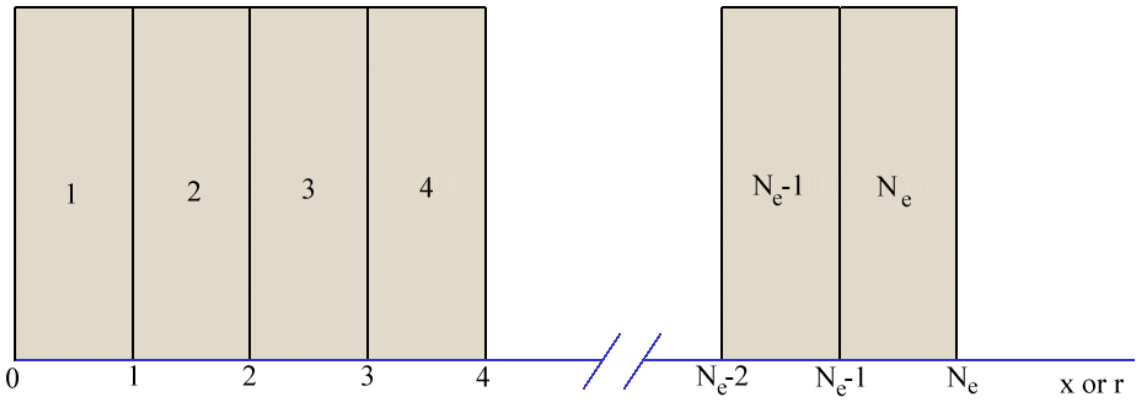

Figure 1.1. Index conventions used in **KB1**.

$$r_i = \sqrt{\frac{R_i^2 + R_{i-1}^2}{2}} \ . \tag{1.3}$$

We express conservation of momentum as an equation of motion for element boundaries. The object is to find the boundary velocities

$$V_i = \frac{dR_i}{dt} \ . \tag{1.4}$$

The time rate-of-change of momentum at boundary *i* equals the time derivative of velocity times half the masses of adjacent elements,

$$\left(\frac{m_{i+1} + m_i}{2} \right) \frac{dV_i}{dt} \ . \tag{1.5}$$

The force on the boundary is the sum of forces from adjacent elements. Summing pressure and magnetic forces gives the equation of motion

$$\left(\frac{m_{i+1} + m_i}{2} \right) \frac{dV_i}{dt} = (-p_{i+1} - w_{i+1} + p_i + w_i)\ 2\pi R_i. \tag{1.6}$$

The new element quantities introduced in Eq. 1.6 are the pressure p_i and artificial viscosity force w_i. The pressure force equals the difference in pressure in the adjacent elements multiplied by the cylindrical area at the boundary. The artificial viscosity force term damps non-physical oscillations at shock fronts. The physical rationale for artificial viscosity and its inclusion in the hydrodynamic equations are covered in Ref. 2. **KB1** employs an adaptation of the von Neumann-Richtmyer form[3,4] used in finite-difference solutions,

$$w = -C\rho\Delta^2 \left|\frac{\partial v}{\partial x}\right| \frac{\partial v}{\partial x}. \tag{1.7}$$

The quantity *C* in Eq. 1.7 is an adjustable parameter with value near unity to spread the shock over several elements, ? is the element scale length, and ?v/?x is the spatial derivative of velocity. KB employs the following difference representation for Eq. 1.7:

$$w_i^n = -C\rho_i^n |V_i^{n-½} - V_{i-1}^{n-½}| \; (V_i^{n-½} - V_{i-1}^{n-½}) \; . \tag{1.8}$$

KB1 advances hydrodynamic quantities using the standard time-centered leap-frog method[12]. The boundary velocities V_i are defined at half time steps and all other quantities apply at integral steps. Throughout this discussion the superscript *n* denotes the time step, so that $t^{n+½} = t^n + ?t/2$. Replacing time derivatives in Eq. 1.6 with time-centered difference operators gives an equation to advance the boundary velocity,

$$V_i^{n+½} = V_i^{n-½} - \left(\frac{\Delta t}{m_{i+1}+m_i}\right) \left[(p_{i+1}^n + w_{i+1}^n - p_i^n - w_i^n) \; 4\pi R_i^n \right] . \tag{1.9}$$

Given the modified velocities, the next step is to advance the boundary radii to the next integral time step,

$$R_i^{n+1} = R_i^n + V_i^{n+½}\Delta t. \tag{1.10}$$

New element densities and average radii can be determined from R_i^{n+1} using Eqs. 1.2 and 1.3.

The internal energy U_i is an element property equal to the material energy of element *i* divided by m_i. The present version of **KB1** does not model changes of U_i resulting from convection or radiation transport. Although straighforward to code, electron thermal conduction contributions

are neglected for three reasons:

- Thermal conduction in solids and liquids is negligible compared to energy transport by shocks.

- Thermal transport coefficients are not well known at high temperature and pressure.

- Energy transport in gases and plasmas is usually dominated by convection.

Under the limiting assumptions changes of internal energy in hydrodynamic calculations result from work performed by pressure, artificial viscosity force and elastic stress. The work performed by pressure and artificial viscosity force on element *i* in a time step is $-(p_i+w_i)\Delta V_i$, where ΔV_i is the change in element volume. The equation to advance internal energy is

$$U_i^{n+1} = U_i^n + \frac{1}{m_i}\left[-\frac{(p_i^{n+1}+p_i^n)}{2} \pi (R_i^{n+12}-R_i^{n2}-R_{i-1}^{n+12}+R_{i-1}^{n\ 2}) \right] . \qquad (1.11)$$

The first term in brackets is a time-centered expression involving the advanced value of pressure. The pressure is estimated by the two-step process described in the next paragraph.

To close the set of equations we must find the new element pressures p_i^{n+1} corresponding to modified values of density and internal energy, ρ_i^{n+1} and e_i^{n+1}. The values are determined from the equation-of-state relationships discussed in Sects. 4 and 7. The KB Tables contain values of pressure and internal energy as functions of density ρ and temperature θ: $p(\rho,\theta)$ and $e(\rho,\theta)$. With known values of density and internal energy the temperature θ can be determined with an inverse interpolation. **KB1** uses a modified two-step method[12] to advance the pressure and preserve time-centering in Eq. 1.11. The advanced internal energy $U_i^{n+1'}$ is first estimated from Eq. 2.11 using only p_i^n. Equation-of-state relations give estimates of the advanced pressure $p_i^{n+1'}$. The quantity $(p_i^n+p_i^{n+1'})/2$ is then substituted in Eq. 2.11 to yield an improved value U_i^{n+1}. Equation-of-state interpolations are repeated to the new pressure p_i^{n+1} and (for materials represented by KB tables) the new temperature $\theta_i^{n+1.}$

Hydrodynamic quantities in KB1		
Symbol	**Description**	**Units**
?	Element density	kg/m^3
r	Average element position	m
R	Element boundary position	m
m	Element mass	kg
V	Element boundary velocity	m/s
?*t*	Time step	s
p	Pressure	Pa ($newtons/m^2$)
w	Artificial viscosity	Pa ($newtons/m^2$)
U	Internal energy	J/kg

---

1. S. Humphries and C. Ekdahl, Laser and Particle Beams **16**, (1998), 405.

2. D. Potter, **Computational Physics** (Wiley, New York, 1973), Chap 9.

3. J. Neumann and R.D. Richtmeyer, J. Appl. Phys. **21** (1950), 232.

4. R.D. Richtmeyer and K.W. Morton, **Difference Methods for Initial-value Problems, Second Edition** (Interscience, New York, 1967).

Section 2. Shock equations

The differential equations for conservation of mass and momentum at a point in a fluid are

$$\frac{\partial \rho}{\partial t} + \nabla\cdot(\rho \boldsymbol{v}) = 0,$$
$$\frac{\partial(\rho \boldsymbol{v})}{\partial t} + \nabla\cdot(\rho \boldsymbol{v}\boldsymbol{v}) = -\nabla p. \tag{2.1}$$

The quantities in Eqs. 2.1 are the density ?, velocity $\boldsymbol{v}$, and pressure p. For a one-dimensional disturbance in the limit of small velocity, the linearized equations are

$$\frac{\partial \rho}{\partial t} = -\rho \frac{\partial v}{\partial x},$$
$$\rho \frac{\partial v}{\partial t} = -\frac{\partial p}{\partial x} = -\frac{\partial p}{\partial \rho}\frac{\partial \rho}{\partial x}. \tag{2.2}$$

The derivative $\partial p/\partial \rho$ is a characteristic of the medium, independent of position and time. Therefore, Eqs. 2.2 imply that

$$\frac{\partial^2 \rho}{\partial t^2} = \left(\frac{\partial p}{\partial \rho}\right)\frac{\partial^2 \rho}{\partial x^2}. \tag{2.3}$$

Equation 2.3 describes small amplitude compression waves that move through the medium at the sound speed

$$C_s = \sqrt{\frac{\partial p}{\partial \rho}}. \tag{2.4}$$

Given an equation of state for the material, we can determine how C_s varies with pressure and density. As an example, consider a ?-law ideal gas[1]:

$$p = A\ \rho^{\gamma}. \tag{2.5}$$

Equation 2.5 implies that the change of pressure with density is

$$\frac{\partial p}{\partial \rho} = C_s^2 = A\ \gamma\ \rho^{\gamma-1}, \tag{2.6}$$

In a perfect gas with ? = 1, the compressibility (and hence the sound speed) is independent of density. Real gases (and most solid and liquid materials) become less compressible at high density because of overlap of electron shells. In this case, ? is greater than unity and hence the sound speed increases with density and pressure. This fact accounts for the existence of shocks.

A *shock* is a sharp discontinuity in density, pressure and temperature that propagates at a well-defined speed u_s through a medium. We can understand the origin of such a discontinuity by considering the excitation of a series of high-amplitude pulsed compressions generated by applying a stair-step pressure waveform on the boundary of a medium. Figure 2.1*a* shows the pressure profile early in time as the compressions propagate into the medium at the sound speed. Because they move through regions of higher pressure and density, pulses produced later in time

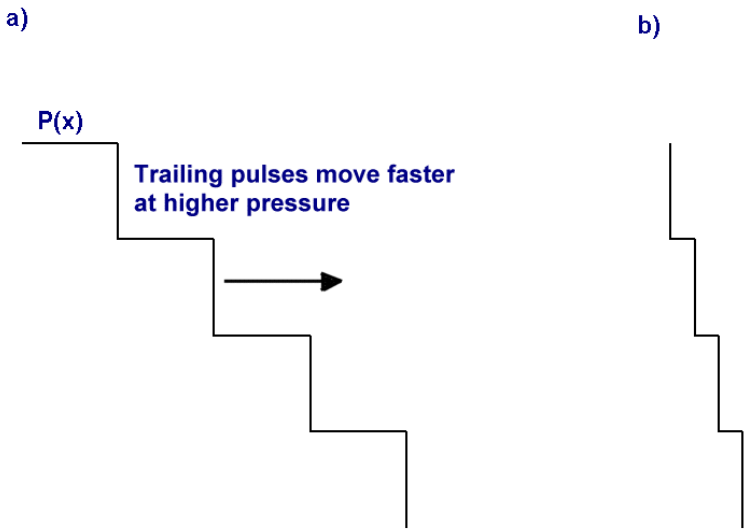

Figure 2.1. Propagation of a high-amplitude pressure waveform at early (*a*) and late (*b*) times.

move faster according to Eq. 2.6. Eventually, they join with the initial pulses to produce a strong localized change in material properties (Fig. 2.1*b*). In other words, the characteristics of wave propagation in the material cause a broad high amplitude pressure waveform applied at the boundary to evolve to a sharp front.

Given the existence of a discontinuity, we can find relationships between material properties before and after passage of the shock by invoking conservation of mass, momentum and energy. Figure 2.2 shows a snapshot of a one-dimensional shock front moving in the +*x*-direction at speed u_s. The undisturbed medium to the right of the front has density $?_o$, pressure p_o and internal energy U_o. We assume that the medium is initially at rest, or the average *x*-velocity of *particles* in the medium is $u_{po} = 0$. We can generalize the derivation by applying a coordinate transformation to a moving frame. The characteristics on the left-hand side of the shock are density $?$, pressure p and internal energy U. The shocked medium has a net average velocity u_p in the +*x*-direction consistent with conservation of mass and momentum. The quantity is usually called the *particle velocity*.

The total mass impinging on the shock from the right equals the total mass leaving to the left. The shock overtakes the undisturbed medium with velocity $-u_s$, so the rate of mass entering the shock per area is $\rho_o u_s$. Material leaves the shock front with apparent velocity $(u_s - u_p)$, so the rate of mass leaving per area is $\rho(u_s - u_p)$. We can write the equation of mass conservation as

$$\rho_o u_s = \rho(u_s - u_p). \tag{2.7}$$

Conservation of momentum implies that the time rate of change of particle momentum per unit area crossing the shock equals the difference in the force per area on each side of the shock. Initially, the particles have zero momentum. Time rate of charge is the rate of mass impinging on the times the final velocity: $(\rho_o u_s)u_p$. The momentum equation can be written

$$p - p_o = \rho_o u_s u_p. \tag{2.8}$$

To express conservation of energy, we equate the rate of work performed by pressure force at the shock to the rate of change of kinetic plus internal energy for mass crossing the shock. In a time $?t$, material occupying a volume per area of $u_s?t$ on the upstream side of the shock changes to a volume per area $(u_s-u_p)?t$ under the influence of a pressure p. The amount of work performed per area equals the pressure times the change in volume per area, or $pu_p?t$. The rate of change of kinetic energy per area equals the mass entering the shock per area times the square of the final velocity or $\rho_o u_s u_p^2$. The rate of change of the internal energy per area equals the mass rate

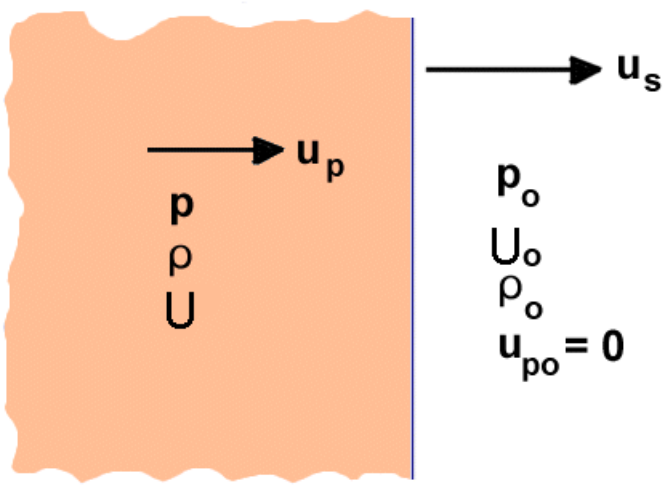

Figure 2.1. Change of quantities at a shock front

entering the shock times the change in energy per mass, or $\rho_o u_s(U-U_o)$. The equation of energy conservation is thus,

$$pu_p = \tfrac{1}{2}\rho_o u_s u_p^2 + \rho_o u_s(U-U_o). \tag{2.9}$$

Equations 2.7, 2.8 and 2.9 involve the known quantities p_o and U_o and the five unknown quantities ?, p, u_s, u_p and U. With an additional equation, we could determine values for four of the unknown quantities in terms of one quantity and thereby generate a family of states that could be achieved by inducing shock waves in materials. The extra relationship is called the *equation of state* (EOS).

Equation 2.9 is often expressed in an alternate form called the *Hugoniot relation*. Solving for the change in internal energy gives,

$$U-U_o = \frac{pu_p - \tfrac{1}{2}\rho_o u_s u_p^2}{\rho_o u_s}. \tag{2.10}$$

Equation 2.8 implies that the particle velocity is $u_p = (p-p_o)/\rho_o u_s$. Substituting in Eq. 2.10, we

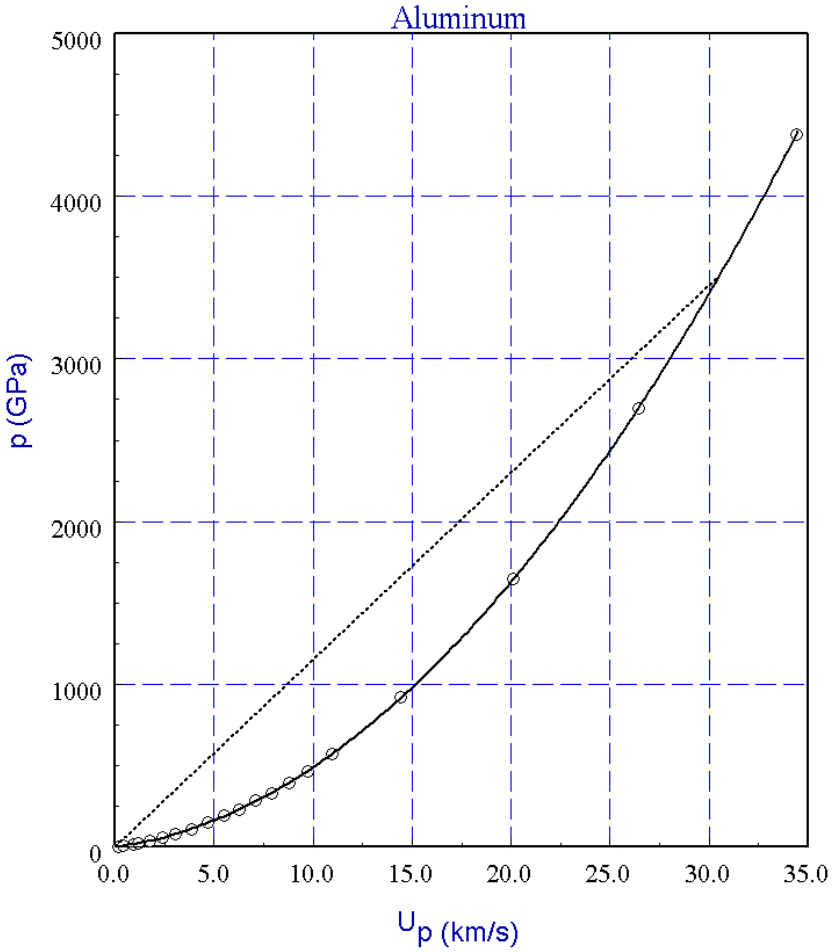

Figure 2.3. Hugoniot plot for aluminum. Marked points calculated by the **KBTView** program.

find that

$$U - U_o = \frac{p(p-p_o) - \frac{1}{2}(p-p_o)^2}{\rho_o^2 u_s^2}. \tag{2.11}$$

Combining Eqs. 2.7 and 2.8 gives the relationship

$$\rho_o^2 u_s^2 = (p-p_o)\,\frac{\rho\rho_o}{\rho-\rho_o}. \tag{2.12}$$

Finally, substituting Eq. 2.12 in Eq. 2.11 gives the Hugoniot relation,

$$U - U_o = \frac{1}{2}\left(\frac{1}{\rho_o} - \frac{1}{\rho}\right)(p - p_o). \tag{2.13}$$

Given an equation-of-state, the shocked material quantities can be plotted as a function of a chosen independent variable. A useful curve is a plot of the change in pressure (p-p_o) versus the particle velocity u_p. Figure 2.3 shows such a plot for aluminum generated from the table `ALUM3715.KBT` using the **KBTView** program with p_o = 0.0 and ?$_o$ = 2700.0 kg/m^3. The curve shows the range of possible final states resulting from a shock. The material changes rapidly from the initial state (origin) to a final state. A straight line on a Hugoniot plot connecting the initial and final states (dashed line in Fig. 2.3) is called a *Rayleigh line*. On a p-u_p plot, the shock velocity can be inferred from the slope of the Rayleigh line. The equation for momentum conservation (Eq. 2.8) implies that

$$\rho_o u_s = \frac{p - p_o}{u_p}. \tag{3.14}$$

The dashed line in Fig. 2.3 connects to a final state with $p = 3.401\times10^{12}$ Pa and $u_p = 3.0\times10^4$ m/s. The predicted shock velocity is 4.199×10^4 m/s. Note that the shape of the curve in Fig. 3.3 implies that u_s increases with the amplitude of the shock.

---

1. R. Courants and K.O. Friedrichs, **Supersonic Flow and Shock Waves** (Springer-Verlag, NewYork, 1991), 7.

Section 3. Shock equations-of-state

For many materials we do not have the full equation-of-state information represented by the KB tables. Fortunately complete information is not required in many useful applications. As an example, consider propagation of a shock. The conservation laws discussed in Sect. 2 limit the range of states that materials can attain. In this case, we can use a simplified equation-of-state that applies only to shock transitions. We must keep in mind that such a model may not provide an accurate description of how the material relaxes after the shock has passed. This limitation does not present a problem for modeling shock-detonated explosives. At detonation the solid explosive rapidly changes to a gas mixture that is well-described by a gamma-law equation of state (Eq. 2.5).

An extensive database of material shock behavior has been generated from experiments. Usually the measured quantities are the shock velocity u_s and the material velocity u_p behind the shock. The relationship between these quantities for a wide variety of materials is well-described by the polynomial relationship,

$$u_s = C_o + S_1 u_p + S_2 u_p^2. \tag{3.1}$$

Given Eq. 3.1 we can substitute in the equations of Section 2 to find all material quantities from any choice of the unknown: ?, p, U, u_s or u_p. Measured data have been collected in several references[1-5].

The **KB** package includes an extensive tabulation of shock equation-of-state data derived from Ref. 3. The file `shockeos.raw` contains measured data for over 400 materials. The file `shockeos.txt` contains values of the parameters C_o, S_1 and S_2 in Eq. 3.1 derived from least-squares fits for all materials where a sufficient number of data points were available. The same information is also available in the spreadsheet files `shockeos.xls` (Microsoft Excel) and `shockeos.qpw` (Quattro Pro 9.0). All quantities are in SI units. Two additional quantities are included. The first, *Stdv*, is the standard deviation of measured values of u_s about the fitted curve. It indicates the variations in the experimental data. The second quantity, *upmax*, is the maximum measured value of u_p. Use of the fitted curve beyond this point involves extrapolation.

The quality of available data varies considerably. For example, Figure 3.1 shows the data points and fit for solid copper. As with most metals, the $u_s(u_p)$ curve is almost a straight line. Figure 3.2 shows an exception, the curve for antimony. Figure 3.3 shows data for the explosive

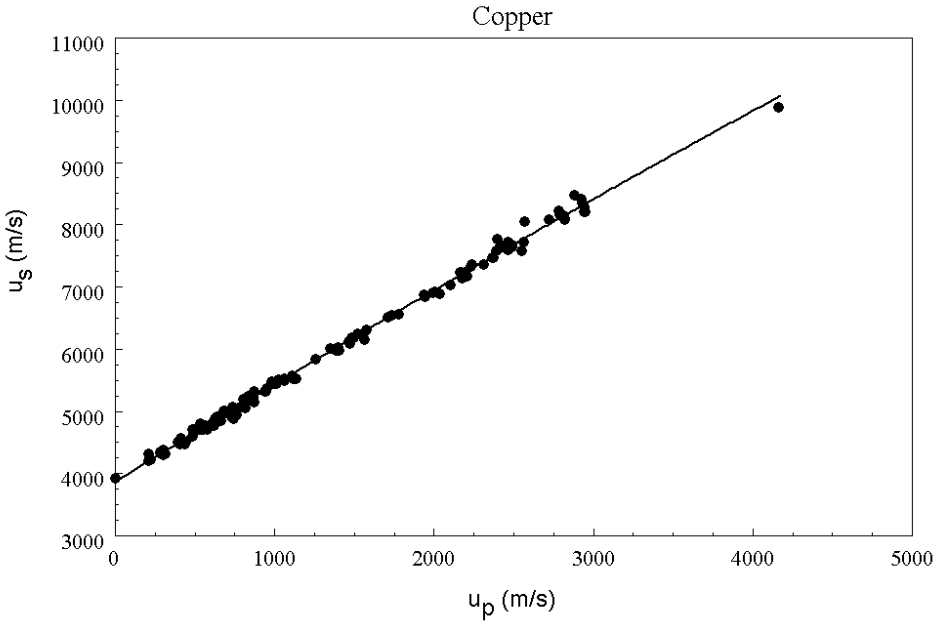

Figure 7.1. Least-squares fit to the data for copper in Ref. 3

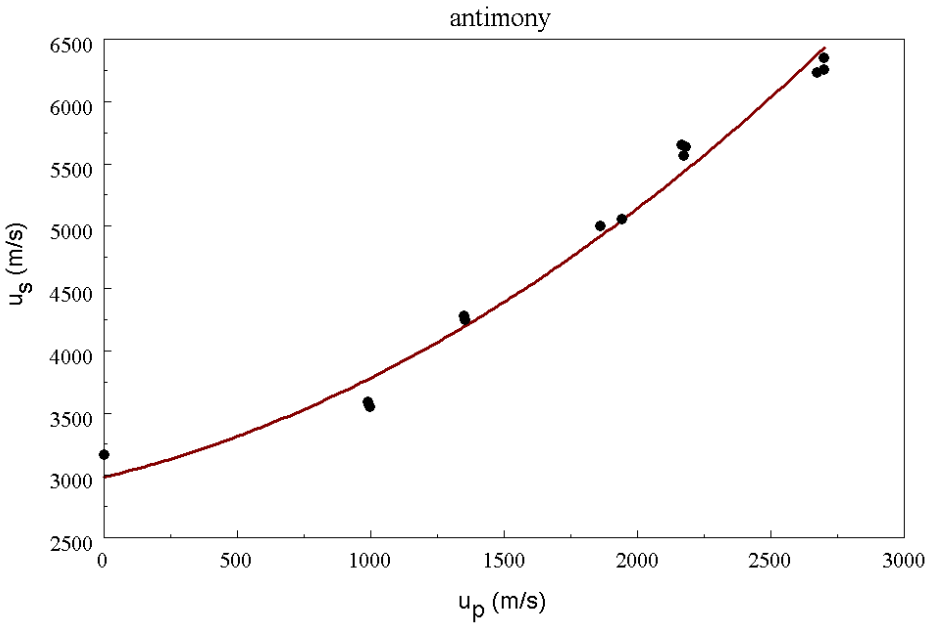

Figure 7.2. Least-squares fit to the data for antimony in Ref. 3

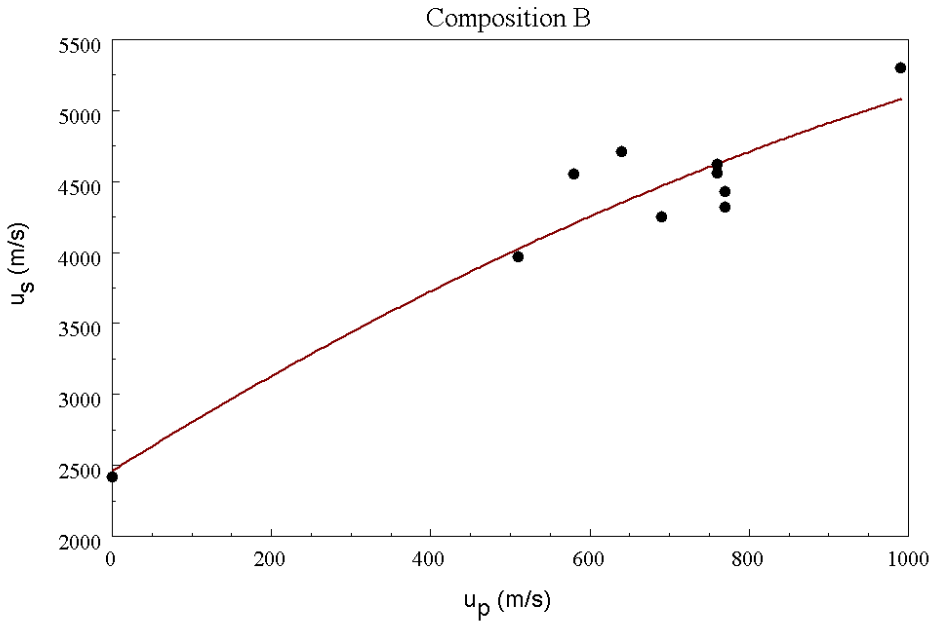

Figure 7.3. Least-squares fit to data of Ref. 3 for Composition B.

Composition B. Understandably, fewer data points are available. There could be significant errors for extrapolations beyond u_p = 1000 m/s.

As described in Sect. 1, we need a function of the form p(?,*U*) to close the hydrodynamic equations used in the **KB** codes. We can derive such a relationship for materials undergoing a shock transition by combining Eq. 3.1 with the equations of Section 2. The Hugoniot relation can be written

$$U - U_o = \frac{1}{2}\left(\frac{\rho\rho_o}{\rho - \rho_o}\right)(p - p_o). \tag{3.2}$$

Substituting for (p-p_o) from Eq. 2.8 gives

$$U - U_o = \frac{1}{2}\left(1 - \frac{\rho_o}{\rho}\right) u_s u_p. \tag{3.3}$$

The mass conservation equation implies that

$$\frac{\rho}{\rho_o} = 1 - \frac{u_p}{u_s}. \tag{3.4}$$

Combining Eqs. 3.3 and 3.4,

$$U - U_o = \tfrac{1}{2}\, u_p^2, \tag{3.5}$$

or

$$u_p = \sqrt{2(U - U_o)}. \tag{3.6}$$

Given u_p, we can find u_s from Eq. 3.1. Application of the energy equation (Eq. 2.9) gives an expression for the pressure:

$$p = \rho_o u_s \left(\frac{u_p}{2} + \sqrt{\frac{U - U_o}{2}} \right). \tag{3.7}$$

Equations 3.6 and 3.7 involve differences in internal energy, U-U_o. The convention in **KB** is to take U_o ? 0 for materials described by the shock equation-of-state.

Another type of material model used in the **KB** codes is the gamma-law gas (Eq. 2.5). In this case, the pressure is given by

$$p = (\gamma - 1)\, \rho_o\, U. \tag{3.8}$$

1. M.H. Rice, R.G. McQueen and J.M. Walsh, Sol. State Phys. **6** (1958), 9,

2. R.G. McQueen, S.P. Marsh, J.W. Taylor, J.N. Fitz and W.J. Carter, in R. Kinslow (*ed*.), High-velocity Impact Phenomena (Academic Press, New York, 1970), 299.

3. S.P. Marsh (*ed.*), **LASL Shock Hugoniot Data** (University of California Press, Berkeley, 1980).

4. C.E. Anderson, J.S. Wilbeck, J.C. Hokanson, J.R. Asay, D.E. Grady, R.A. Graham and M.E. Kipp in Y.M. Gupta (*ed*.), **Shock Waves in Condensed Matter - 1985** (Plenum Press, New York, 1986).

5. D.J. Steinberg, *Equation-of-state and Strength Properties of Selected Materials* (Lawrence Livermore National Laboratory, Report UCRL-MA-106439, 1991), unpublished.

Section 4. Detonation physics

Explosive materials release chemical energy at a very high rate. In the process of *detonation*, a solid or liquid explosive rapidly changes to a gas in a highly compressed state. During expansion the gas can perform a considerable amount of work. The quantity Q denotes the chemical energy released. Typical explosives have Q values of about 5 MJ/kG. Practical explosives have a high activation energy so that they do not spontaneously ignite. The required energy to initiate detonation is about 150 kJ/mole. For typical explosives the specific activation energy is about U_a = 0.5 MJ/kG. Ignition of an explosive material is usually performed by a detonator that generates a shock on the surface. The shock has sufficient amplitude to raise the internal energy by an amount exceeding U_a. The resulting rapid transformation of the material amplifies the shock which moves into adjacent regions. The process leads to a self-sustained detonation front that consumes the explosive material.

The detonation model used in **KB1** and **KB2** is straightforward[1]. Before detonation the properties of explosive materials are determined from the shock equation-of-state model discussed in Sect. 3. If the pressure in an element of explosive material exceeds a threshhold value P_{init}, the element detonates. At detonation the code augments the internal energy of the element by Q and subsequently determines the element pressure from the gamma law equation of state (Eq. 3.8). An underlying assumption is that the chemical reaction occurs rapidly in comparison to the propagation time for the detonation front.

The following parameters are required for a complete description of an explosive material in **KB1** and **KB2**:

- ? o. The density of the solid material under ambient conditions (kg/m3)

- C_o,S_1 and S_2. Parameters in the $u_s(u_p)$ relationship, tabulated in the resources discussed in Sect. 7 and in Appendix 2.

- P_{init}. The threshhold pressure for detonation (Pa).

- Q, the specific energy released by the chemical reaction (J/kg).

- ?, constant for the gas equation-of-state.

The quantities $?_o$, Q and ? are tabulated in the file explode.txt for several materials. Additional data can be found in the references listed at the end of this section.

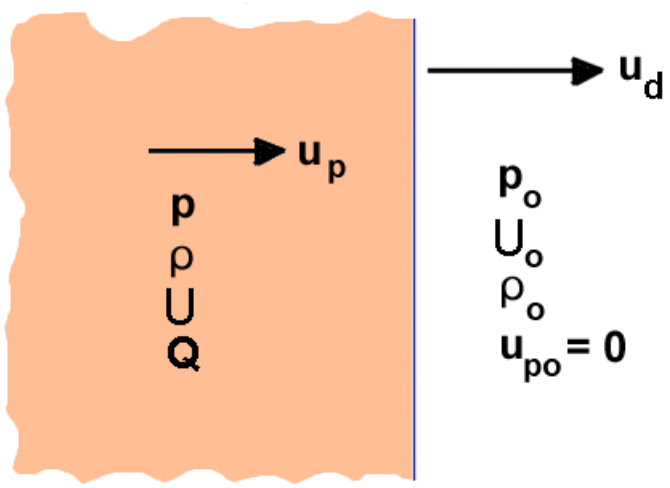

Figure 4.1. Quantities at a detonation front

It is useful to review the equations for a one-dimensional detonation in a homogeneous material in order to understand the underlying physics and to define benchmark tests for the **KB1** and **KB2** codes. Figure 4.1 shows the geometry. A self-sustained front moves into an ambient explosive at a velocity u_d. The undisturbed material at rest has properties ?$_o$, p_o, U_o and $u_{po} = 0$. The gaseous material behind the front has density ?, pressure p, internal energy U, and a directed velocity u_p. We can determine unique values for the material state behind the front in terms of the properties of the explosive by applying conservation of mass, momentum and energy at the discontinuity. With the exception of the chemical energy released, the equations are the same as those derived in Sect. 2. The equation for conservation of mass is

$$\rho_o u_d = \rho(u_d - u_p), \tag{4.1}$$

and conservation of momentum is given by

$$p - p_o = \rho_o u_d u_p. \tag{4.2}$$

To express conservation of energy, we include the specific chemical energy in Eq. 3.5:

$$U - U_o = \tfrac{1}{2} u_p^2 + Q. \tag{4.3}$$

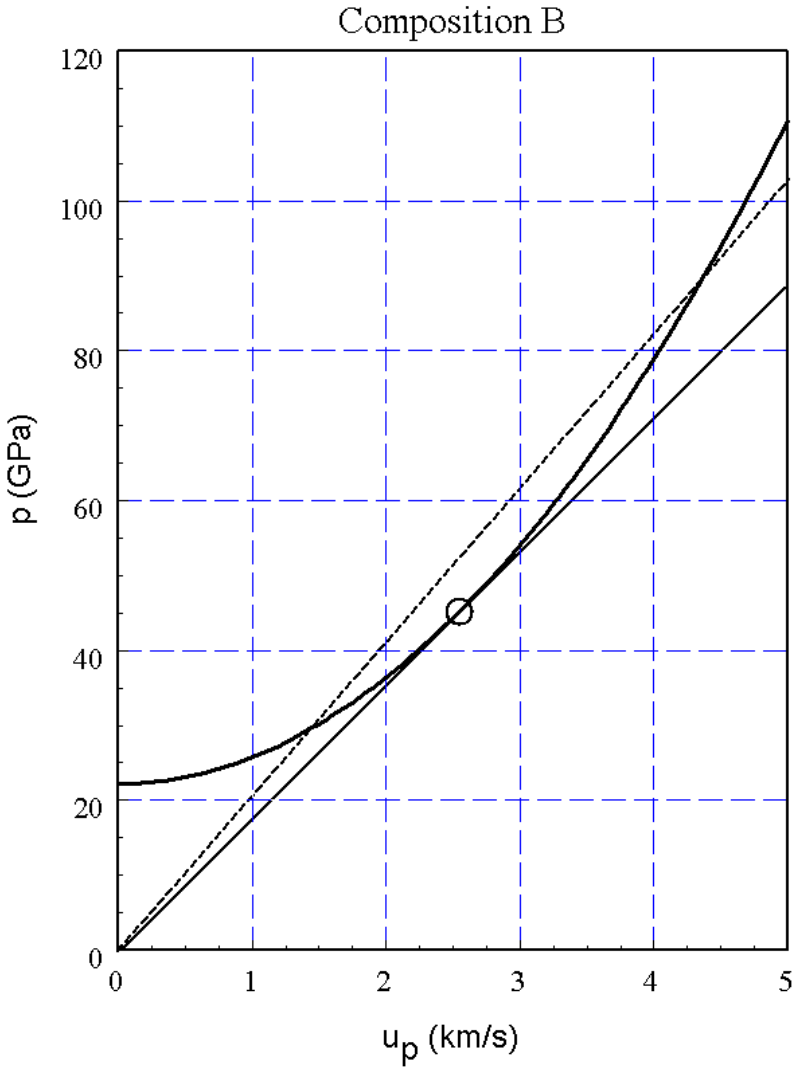

Figure 4.2. Determination of the Chapman-Jouguet point

To simplify the equations, we assume that the initial pressure p_o and internal energy U_o are negligible compared to the values in the detonated state. Furthermore, we assume that the properties of the detonated material are governed by the gamma law equation-of-state:

$$p = (\gamma - 1)\, \rho_o\, U. \tag{4.4}$$

The momentum equation (Eq. 4.2) implies that following relationship for the detonation velocity:

$$u_d = \frac{p}{\rho_o u_p}. \tag{4.5}$$

We can combine Eqs. 4.1 through 4.4 to derive an expression for the material pressure in terms of the particle velocity,

$$p = \tfrac{1}{2}\,\rho_o\,(\gamma+1)\,u_p^2 + \rho_o\,Q\,(\gamma-1). \tag{4.6}$$

Figure 4.2 shows a plot of Eq. 4.6 for Composition B (ρ_o = 1770.0 kg/m^3, Q = 6.270×10^6 J/kg and γ = 3). The plot represents an infinite set of possible states consistent with the explosive properties and conservation laws. The slope of a line connecting a point on the curve to the origin (dashed line in Fig. 4.2) implies a value of the detonation velocity according to Eq. 4.5. Note that there is an ambiguity for the dashed line illustrated. The same value of u_d corresponds to two different final states. The only possible unique state is shown by the solid line tangent to the curve, corresponding to the minimum value of u_d. This material state, the *Chapman-Jouguet point*[2-3], is the correct representation for a detonation front[4].

We can find material properties at the Chapman-Jouguet point by combining Eqs. 4.5 and 4.6 to determine u_d in terms of u_p:

$$u_d = \frac{(\gamma+1)\,u_p}{2} + \frac{(\gamma-1)Q}{u_p}. \tag{4.7}$$

Setting $du_d/du_p = 0$ gives the particle velocity at the Chapman-Jouguet point as:

$$u_p(CJ) = \sqrt{\frac{2Q(\gamma-1)}{\gamma+1}}. \tag{4.8}$$

Inserting Eq. 8.8 in Eq. 8.6 gives the Chapman-Jouguet pressure

$$p(CJ) = 2\,\rho_o\,Q\,(\gamma-1). \tag{4.9}$$

Inserting the values u_p(CJ) and p(CJ) into Eq. 4.5 gives the detonation velocity,

$$u_d = \sqrt{2\,Q\,(\gamma - 1)\,(\gamma + 1)}. \qquad (4.10)$$

The parameters of Composition B used in Fig. 4.2 imply that u_p(CJ) = 2.50 km/s, p(CJ) = 44.39 GPa, and u_d = 10.0 km/s.

---

1. Adapted from M.A. Meyers, **Dynamic Behavior of Materials** (Wiley, New York, 1994), Chap 10.

2. D.L. Chapman, Lond. Edinb, Dubl. Phil. Mag. **47** (1899), 90.

3. E. Jouguet, J. Math. Pure Appl. **60** (1905) 347, **61** (1906), 1.

4. The rationale for the Chapman-Jouguet condition is not intuitively obvious. A detailed discussion is given in J. Taylor, **Detonation in Condensed Explosives** (Clarendon Press, Oxford, 1952), 69-78.

Section 5. Two-dimensional hydrodynamics on a triangular mesh

The numerical treatment of the hydrodynamic equations in **KB2** is based on the division of the solution volume into small elements. The elements have a triangular shape so that they conform closely to boundaries in the initial system and can flex to follow changes in the geometry of the medium. Elements have a unique material identity that does not change during the simulation. On the other hand, the position, shape and size of elements may vary. The hydrodynamic quantities (pressure, density, temperature and internal energy) also vary. The finite-element approach is closely related to the Lagrangian viewpoint for finite-difference calculations. The calculation is referenced to materials rather than to a fixed coordinate system.

The computational approach in **KB2** has several advantages:

- The physical motion automatically refines the mesh - the code gives good results for systems that undergo substantial compression or expansion,
- The conformal mesh accurately represents curved or slanted material boundaries,
- The element-centered view helps in modeling complex processes like detonation.
- Unspecified boundaries automatically represent unconstrained material with free expansion.

On the other hand, **KB2** has drawbacks so it may not be practical for all problems. During a simulation it is essential to maintain the logical connections of the mesh. The implication is that elements that are initially neighbors must remain adjacent. Because **KB2** maintains continuity of phase space, it is not well-suited to systems that disassemble, cavitate or mix. Simulations terminate when elements are stretched to the breaking point (*i.e.*, logical inversion of a triangle). Similarly, it is difficult to represent systems with initially separated objects (*i.e.*, a shaped projectile striking a surface).

In **KB2** the term *element* refers to the area inside a triangle while the term *node* applies to the triangle vertices. Three quantities are associated with nodes: position ([x,y] or [r,z]), velocity ([v_x,v_y] or [v_r,v_z]) and mass (M). The remaining quantities are taken as properties of the elements: pressure (P), temperature (T), density (?), internal energy (?) and artificial viscosity ([w_x,w_y] or [w_z,w_r]). The code solves equations of motion for nodes to infer changes in the element size and shape. The change in element volume is then used to update the hydrodynamic quantities. In the **TriComp** mesh every internal node is surrounded by six elements as in Fig. 5.1. In the figure, elements and nodes surrounding the central node are labeled 1-6. The path shown in blue passes

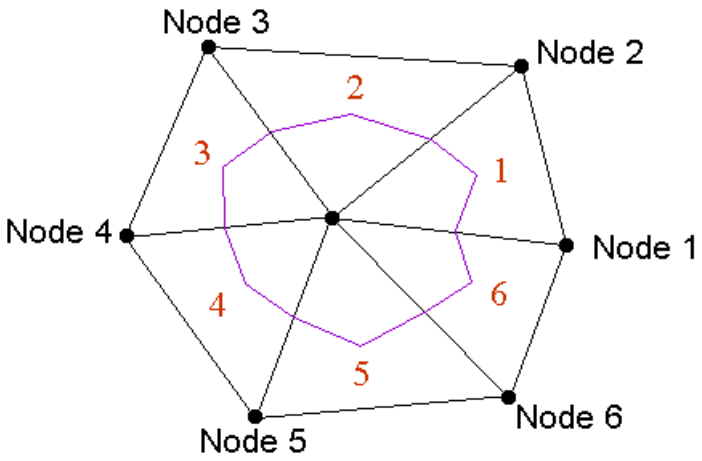

Figure 5.1. Elements and nodes surrounding an internal node

through the centers of lines connecting neighboring nodes and the centers-of-mass of the elements. The path encloses one-third of the element areas. We set the node mass M equal to the mass inside the path (one-third of the mass of the six elements). The element mass equals ? multiplied by the element volume. The node masses are invariant because the element masses are conserved.

The force on a vertex arises from the pressure and artificial viscosity of surrounding elements. The total force on a node is determined is determined from an integral of pressure over the surrounding surface shown in Fig. 5.1. After some algebra, the integration yields a simple and intuitive result. In planar geometry, the expression for pressure force (per length in *z*) is:

$$F_x = -\tfrac{1}{2}\left[P_1(y_1-y_6) + P_2(y_2-y_1) + P_3(y_3-y_2) + P_4(y_4-y_3) + P_5(y_5-y_4) + P_6(y_6-y_5)\right],$$

$$F_y = \tfrac{1}{2}\left[P_1(x_1-x_6) + P_2(x_2-x_1) + P_3(x_3-x_2) + P_4(x_4-x_3) + P_5(x_5-x_4) + P_6(x_6-x_5)\right].$$

The quantities (x_i,y_i) are the coordinates of the surrounding nodes.

At each integer time step **KB2** determines the force components at a node from values of pressure and artificial viscosity in surrounding elements. The equation of motion is used to determine new values of node velocities at the half-integer time step. The velocities are then used to advance the node positions to the next integer time step. The node positions are then used to find new element volumes in planar or cylindrical geometry. A new value of internal energy ? can be determined from the change of volume and other possible processes (such as detonation) . Finally, the new density ? and internal energy can be used to determine the pressure through the

equation-of-state for the element material. The procedure is applied to all elements and continues over subsequent time steps.

Although the method is simple in principle, there are several challenges in the practical application, including:

- representation of applied pressures over arbitrary boundaries,
- implementation of symmetry boundaries (sliding surfaces),
- determination of methods for cylindrical systems that maintain good accuracy near the axis.
- addition of artificial viscosity contributions on arbitrary triangular meshes.
- organization of multiple materials and regions.